Subsurface Evolution and Persistence of Marine Heatwaves in the Northeast Pacific

H. A. Scannell[1], G. C. Johnson[2], L. Thompson[1], J. M. Lyman[2,3], S. C. Riser[1]

[1]School of Oceanography, University of Washington, Seattle, WA, USA.

[2]Pacific Marine Environmental Laboratory, NOAA, Seattle, WA, USA.

[3]Joint Institute for Marine and Atmospheric Research, University of Hawaii at Manoa, Honolulu, HI, USA.

Corresponding author: Hillary A. Scannell (scanh@uw.edu)

Key Points :

- Return of The Blob, with warming and freshening, hence more buoyancy.
- Summertime heatwaves, increase stratification, inhibit mixing.
- Wintertime mixing, warming penetrates the deep, provides memory.

Abstract

The reappearance of a Northeast Pacific marine heatwave (MHW) sounded alarms in late summer 2019 for a warming event on par with the 2013–2016 MHW known as The Blob. Despite these two events having similar magnitudes in surface warming, differences in seasonality and salinity help to distinguish their evolution. We compare and contrast the ocean's role in the evolution and persistence of the 2013–2016 and 2019–2020 MHWs using mapped temperature and salinity data from Argo floats. An unusual near-surface freshwater anomaly in the Gulf of Alaska during 2019 increased the stability of the water column, preventing the MHW from penetrating as deeply as the 2013–2016 event. The freshwater anomaly in 2019 likely contributed to the intensification of the MHW by increasing the near surface buoyancy. The gradual buildup of subsurface heat content throughout 2020 in the region suggests the potential for persistent ecological impacts.

Plain Language Summary

Marine heatwaves (MHWs) are periods of prolonged and unusually warm regional sea surface temperature that can negatively impact the health and productivity of marine ecosystems. Using surface and subsurface ocean observations, we compare and contrast two recent MHWs to show that salinity variations play an important role in the vertical distribution of temperature anomalies by changing the overall stability of the water column. During the 2019–2020 MHW, the near-surface waters in the Gulf of Alaska were fresher than normal, preventing warm sea surface temperatures from mixing as deeply into the subsurface as in the 2013–2016 MHW. The freshening in 2019 likely enhanced warming in the buoyant surface layer. As warmer temperatures gradually mix downward they can persist long after the surface MHW disappears, suggesting that the ocean can provide memory for long-lived MHWs. The subsurface persistence of MHWs has potential ramifications for long-lasting ecological impacts.

1 Introduction

Marine heatwaves (MHWs) have become distinguishable features of Northeast (NE) Pacific temperature variability that disrupt the productivity of marine ecosystems and their services (Smale et al., 2019). These prolonged, discrete, and anomalously warm water events (Hobday et al., 2016) are most recognizable at the sea surface, where the effects of ocean warming have led to a near-doubling in the average annual count of MHW days globally since the early 20th Century (Oliver et al., 2018). Although MHWs have occurred throughout the global ocean, the NE Pacific has recently emerged as a hotspot for extremely persistent and large-scale events that are forced by anomalous air-sea heat flux driven by remote forcing from the tropics, in addition to long-term warming from anthropogenic greenhouse forcing (Holbrook et al., 2019). The most remarkable NE Pacific MHWs have occurred in 2013–2016 and 2019–2020, and are colloquially referred to as The Blob (Bond et al., 2015) and Blob2.0 (Amaya et al., 2020) respectively (Figure 1 and Figure S1).

The strength of sea surface temperature (SST) anomalies associated with MHWs depends critically on the seasonal evolution of the mixed-layer depth (MLD), which deepens in winter and shoals in summer. If MHW anomalies are present in the spring when the NE Pacific MLD shoals, they can become trapped in the subsurface during the summer through detrainment. These detrained SST anomalies are then stored in the subsurface and can reemerge the following winter when the MLD deepens and re-entrains those stored anomalies (Alexander et al, 1999). Alternatively, in the presence of downward Ekman pumping from wind stress curl, for example in the North Pacific subtropical gyre, detrained anomalies can subduct, where they are further isolated from the mixed layer (Qiu and Haung, 1995). Here, we explore the role of detrainment and subduction in the sequestration of MHW anomalies into the permanent pycnocline where they can persist for years.

During the 2013–2016 NE Pacific MHW, lower rates of wintertime turbulent heat loss from the ocean to atmosphere and a reduction in wind-generated stirring allowed the winter mixed layer to remain unseasonably warm and shallow in the south central region of the Gulf of Alaska (Bond et al., 2014). As the 2013–2016 NE Pacific MHW progressed, local positive downward shortwave radiation and a positive SST-cloud feedback over the Southern California Current System reinforced surface warming near the coast almost one year later (Schmeisser et al., 2019; Zaba and Rudnick, 2016). Below the mixed layer, anomalously warm and salty water was detrained to denser and deeper isopycnals to depths of at least 150 m (Jackson et al., 2018). These subsurface anomalies lingered through 2017, long after the initial onset of atmospheric forcing.

A similar situation played out during the summer of 2019 when a resurgence of Blob-like surface conditions intensified in the NE Pacific. Weakened surface wind speeds, forced by teleconnections associated with SST anomalies in the Tropical Pacific, resulted in reduced evaporative heat loss from the ocean to atmosphere and limited wind-driven mixing, resulting in a MHW off the U.S. West Coast (Amaya et al., 2020). Increased shortwave radiation and a positive SST-cloud feedback helped to maintain the MHW over an exceptionally shallow summertime mixed layer (Amaya et al., 2020). Here, we find evidence for the propagation and persistence of the 2019–2020 NE Pacific MHW in the subsurface, which may help prolong the impacts of MHW-like conditions into 2021.

In this study, we examine the connections between surface MHWs and the subsurface structure of temperature, salinity, and density by analyzing objectively mapped monthly Argo data in the NE Pacific, comparing and contrasting the 2013–2016 and 2019–2020 MHWs. We characterize the spatiotemporal evolution of anomalous subsurface conditions and their connection to mixed layer properties from January 2004 through June 2020, and we quantify the change in water mass properties and ocean heat content anomalies within and below the mixed layer. Understanding the subsurface evolution and persistence of MHWs gives insight into the potential predictability and reemergence of these events in the future, where a trend towards shallower summertime MLDs is expected to increase the likelihood and frequency of MHWs in the North Pacific (Amaya et al. in review). The persistence and potential reoccurrence of MHWs could result in long-lasting impacts on the health of marine ecosystems, especially in the subsurface where the effects of warming on marine life (i.e., thermal stress) can persist for years (Cavole et al., 2016).

2 Data

We analyze monthly mean SST maps from the Optimum Interpolation SST version 2 (OISSTv2) dataset on a 0.25º longitude by 0.25º latitude global grid from 1982 through present (Reynolds et al., 2002; 2007). These SST maps are generated from a blend of satellite (Advanced Very High Resolution Radiometer only), ship, buoy (both moored and drifting), and Argo float data. The satellite data are interpolated to fill gaps and are bias corrected with reference to buoys to account for platform differences. We use the OISSTv2 dataset as it incorporates *in situ* observations, offers complete global eddy-resolving coverage, and spans almost 40 years.

We also analyze monthly mean fields from January 2004 through June 2020 from the updated Roemmich-Gilson Argo Climatology (Roemmich and Gilson, 2009; hereafter RG09) to examine the vertical structure of temperature, salinity, and density anomalies associated with MHWs. Argo is a global network of autonomous profiling floats that continuously measures the temperature and salinity of the upper 2,000 m of the ocean. The Argo program began in 1999 and now consists of over 3,800 active floats and more than 2 million hydrographic profiles reported thanks to a coordinated effort from dozens of countries worldwide (Jayne et al., 2017). Archived and near real-time float data are made publicly available (http://sio-argo.ucsd.edu/RG_Climatology.html) and are incorporated into monthly maps on a 1º longitude by 1º latitude grid beginning in January 2004 when the global array had at least 1,000 floats and first approached sparse global coverage (RG09). These maps are made in 58 pressure layers with the shallowest centered on 2.5 dbar and the deepest on 1,975 dbar, with finer resolution near the surface (e.g., spaced 10 dbar apart from 10 to 170 dbar). The 2.5 dbar temperature anomaly in RG09 closely tracks the OISSTv2 in the NE Pacific, capturing large scale spatial and temporal variability.

In addition to the mapped temperature and salinity vs. pressure fields from RG09, we also analyze 19,697 quality-controlled Argo profiles in the NE Pacific (35.5–51.5ºN, 135.5–154.5ºW; box in Figure 1) to compute the MLD from January 2004 through June 2020 using the density algorithm from Holte and Talley (2009). The sampling frequency from Argo in the NE Pacific (35.5–51.5ºN, 135.5–154.5ºW) steadily increases from the early 2000s, achieving over 1,000 profiles per year starting in 2012 (Figure S2). These profiles were downloaded from one of the two Argo Global Data Assembly Centers (https://nrlgodae1.nrlmry.navy.mil/argo/argo.html) in August 2020.

3 Analysis

We define MHWs locally when SST exceeds the monthly climatological 90th percentile from January 2004 through June 2020. Our definition for MHWs is similar to that proposed in Hobday et al. (2016) with modification in the length of the climatological period and in the minimum event duration. Owing to the prominence and persistence of the 2013–2016 and 2019–2020 MHWs, our definition highlights the same large-scale features described in previous studies using daily data (e.g., Fewings and Brown, 2019; Gentemann et al., 2017).

Before analyzing the RG09 dataset, we fit temperature and salinity at each spatial point to the mean, trend, annual, and semiannual harmonics using least squares regression from January 2004 through June 2020. We then remove the mean, annual, and semi-annual harmonics (but not the trend) to generate anomalies. We smooth these anomalies and the regression coefficients with a 5-month Hanning filter and then a 6° latitude x 6° longitude LOESS filter to reduce mesoscale signals that are retained in the RG09 maps. We then reconstruct the total smoothed in-situ temperature and practical salinity maps using the smoothed anomalies and smoothed model coefficients. We apply the thermodynamic equation of seawater (Intergovernmental Oceanographic Commission et al., 2010) to compute the absolute salinity (S_A) and conservative temperature (Θ) at each space and time grid point. Using S_A and Θ, we also compute the potential density anomaly (σ_θ) with reference to 0 dbar; expressed as a particular potential density minus 1000 kg m^{-3}. The potential density represents the density a fluid parcel would acquire if it were brought adiabatically to the sea surface, thus eliminating the density dependence on pressure. We also map the RG09 fields of S_A, Θ, and pressure (P) to a vertical density coordinate, σ_θ. We compute anomalies in S_A, Θ, and P in σ_θ coordinates, as well as S_A, Θ, and σ_θ in P coordinates, by removing the monthly means of these quantities across the entire 198-month time series at each spatial point and for each vertical coordinate system (σ_θ and P) to get the anomalies.

We examine the ocean heat content anomaly (Q') within the mixed layer (10–90 dbar), thermocline (100–180 dbar), and just below the thermocline (200–280 dbar). We define $Q' = \int \frac{1}{g} \cdot c_p \cdot \Theta' \, dp$, where $g = 9.8\, m\, s^{-2}$ is the acceleration due to gravity, $c_p = 3991.8680\, J\, kg^{-1}\, K^{-1}$ is the standard specific heat of seawater when using Θ, Θ' is the conservative temperature anomaly, and $\int dp$ is the integral over each of these three 80-dbar thick layers.

We apply the Holt and Talley (2009) density algorithm to 19,697 Argo float profiles in the NE Pacific (35.5–51.5ºN, 135.5–154.5ºW; box in Figure 1) to estimate monthly MLDs from January 2004 through June 2020. This method searches for the depth at which the density increases by 0.03 kg m^{-3} relative to a near-surface reference level.

We quantify the bulk stratification of the upper ocean using the Brunt-Väisälä frequency squared $N^2 = \frac{-g}{\rho}\frac{d\rho}{dz}$. Here, $\frac{d\rho}{dz}$ is the change in potential density with reference to 0 dbar between 2.5 and 200 dbar. Large values of N^2 imply an increase in upper ocean stratification that creates a more stable water column. We compute anomalies in N^2, again with respect to monthly long-term means, to quantify the change in the stratification of the upper ocean due to MHW variations in both Θ and S_A.

To further examine the relationships among Θ, S_A, and σ_θ, we examine $\Theta - S_A$ diagrams with contours of constant density and spice to show changes in water-mass properties between different MHW years in the NE Pacific. $\Theta - S_A$ variations along isopycnals can be quantified by spice (Munk, 1981), where warm/salty anomalies are spicy and cool/fresh anomalies are minty. We compute spice following McDougall and Krzysik (2015) using a potential density with reference to 0 dbar. Isopycnal variations in spiciness can be used to describe MHW impacts on isopycnal water-mass properties in density units.

4 Results

Anomalies in $\Theta - S_A$ on isopycnals can be tracked following the surface evolution of SST anomalies during MHWs, and can either be warm/salty (spicy) or cool/fresh (minty), such that the density of that isopycnal does not change (Movie S1). The winter-intensified 2014–2016 MHW had spicy anomalies on 25.4 kg m^{-3}, which lagged the spatiotemporal evolution of SST anomalies within the MHW (hatching in Figure 1). For example, surface MHW conditions moved onshore by late 2014 and began to fade as early as 2015, whereas subsurface spice anomalies did not reach the coast until winter 2015 and persisted into 2016 (Movie S1). By comparison, summer $\Theta - S_A$ anomalies in 2019 lacked the advective nature of the 2013–2016 MHW, yet they were much more widespread. Minty anomalies on 25.4 kg m^{-3} encompassed nearly the entire Gulf of Alaska from late summer 2018 through summer 2020, while spicy anomalies lingered off the coast between Baja California and Hawai'i (Figure 1, Movie S1).

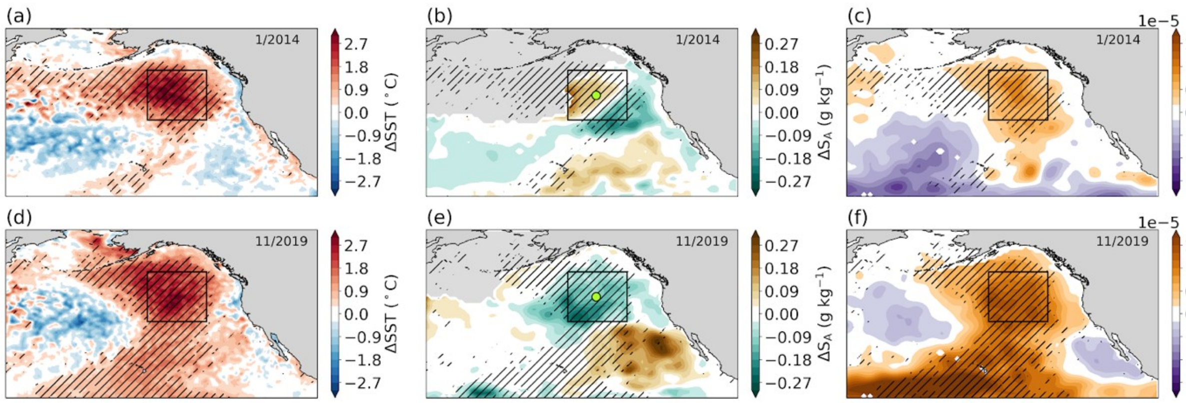

Figure 1. Spatial characteristics of NE Pacific MHWs during January 2014 (a-c) and November 2019 (d-f); the two warmest months of SST anomalies averaged in the boxed region from 2004 through 2020. First column (a,d) shows SST anomalies from the OISSTv2 where diagonal hatching indicates the locations experiencing a MHW. Hatching across columns is consistent. The middle column (b,d) is the absolute salinity anomaly on 25.4 kg m^{-3}. By definition, conservative temperature anomalies mirror salinity anomalies on isopycnals where conditions are either warm/salty or cool/fresh. The third column (c,f) shows the bulk upper ocean stability anomaly in terms of the Brunt-Väisälä frequency squared computed using the anomalous density difference between 2.5 and 200 dbar. All anomalies are referenced to the January 2004 through June 2020 monthly climatology. The bounding black box represents the area defined by 35.5–51.5ºN, 135.5–154.5ºW and the lime green circles in (b) and (c) mark 43.5ºN, 145.5ºW.

Positive stratification (N^2) anomalies occurred for both the 2013–2016 and 2019–2020 MHWs, however were much greater in 2019 (Figure 1, Movie S1). Warm and fresh near-surface anomalies in 2019 decreased density and increased the stratification (Figure 2), whereas in 2013–2016 the near-surface density reduction from a warm anomaly was partially offset by a salty anomaly. The increase in pressure along 25.4 kg m^{-3} beginning in 2018 reflects an increase in stratification even before the onset of the 2019 MHW (Figure 2). The 2019 large and positive stratification anomaly likely inhibited the surface MHW from penetrating as deeply as the 2013–2016 MHW, and furthermore may have enhanced the surface build-up of heat.

Prior to 2013, two other noteworthy MHWs occurred in the NE Pacific from 2004–2005 and 2008–2009 (Figure 2). Warm subsurface *Θ* anomalies during these MHWs extended and propagated to depths of about 200 m and anomalies at 25.4 kg m^{-3} were spicy, similar to that of the 2013–2016 event. Warm and salty anomalies reduced subsurface density and increased the stratification of the surface layer. The 2004–2005 MHW was more stratified than the 2008-2009 event owing to the larger surface density anomaly (Figure 2e and Figure 5b-c).

The near-instantaneous deep anomaly in 2008–2009 below 150 dbar likely resulted from adiabatic motions caused by isopycnal heave, as indicated by the downward deflection of 26.3 kg m^{-3} (Figure 2a). Heave occurs in response to Ekman pumping due to wind stress curl that depresses the main thermocline (Bindoff and McDougall, 1994). Positive pressure anomalies on 26 kg m^{-3} indicates a deepening of the thermocline in 2008–2009 at approximately 130 dbar (Figure 2f). These vertical isopycnal motions are adiabatic, meaning there is no exchange of heat or salinity with the surrounding environment (i.e., no diapycnal mixing occurs), so water mass properties are conserved. As a result, warm and fresh anomalies in 2008–2009 occurred along the 150–200 isobars, however, were negligible on 26.3 kg m^{-3}, which migrates annually between 150–200 dbar (Figure 2).

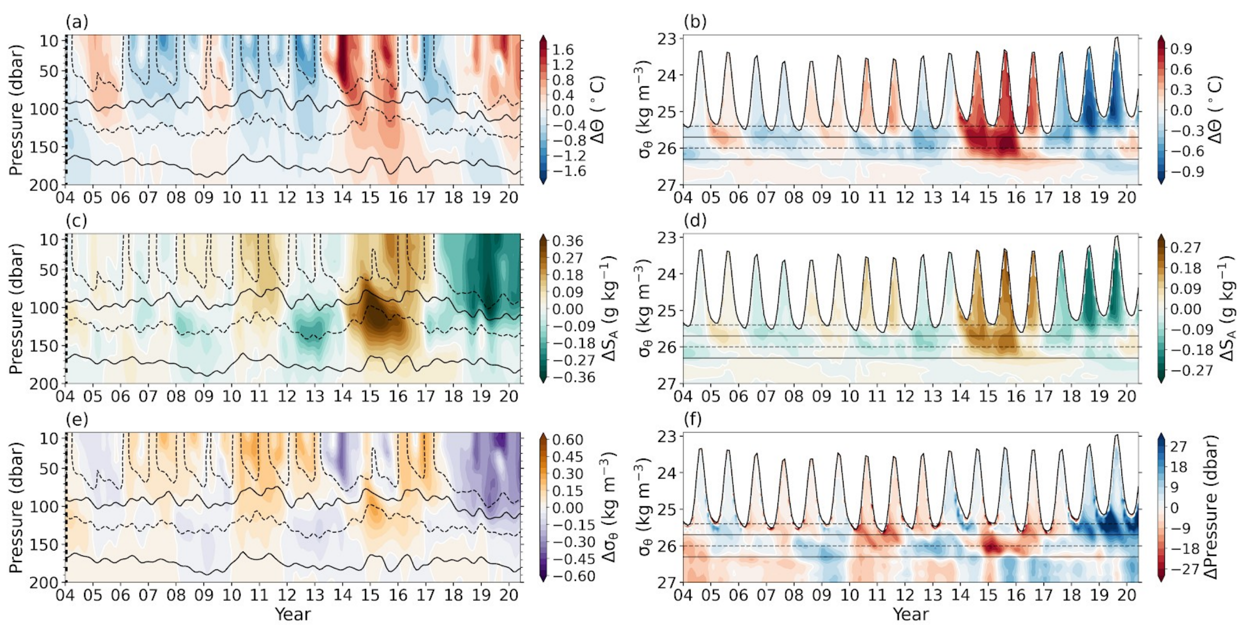

Figure 2. Progression of monthly anomalies in (a,b) conservative temperature, (c,d) absolute salinity, (e) potential density, and (f) isopycnal pressures at 43.5ºN, 145.5ºW (lime green circles in Figure 1) from January 2004 through June 2020. Contours of the 25.4 kg m^{-3} (upper dashed),

25.7 kg m^{-3} (upper solid), 26 kg m^{-3} (lower dashed), and 26.3 kg m^{-3} (lower solid) isopycnal surfaces vary with pressure (a,c,e), however are constant when plotted against density (b,d,f).

Analysis of $\Theta - S_A$ relationships along isopycnals provide additional insight into water-mass property changes during MHWs. Here, spice is primarily controlled by the exchange of heat and freshwater between the ocean and atmosphere, ocean turbulent mixing, and lateral advection. Spicy conditions occurred each winter (December-January-February) during the 2013–2016 MHW, most notably in waters lighter than 26.5 kg m^{-3} during the winters of 2014/15 and 2015/16 (Figure 3a). The warmest wintertime temperatures occurred in 2013/14 where $\Theta - S_A$ variations were confined to lighter isopycnals (<26 kg m^{-3}). Winter spice anomalies in 2013/14 likely mixed into the permanent halocline to denser isopycnals by summer, as can be seen along 25.6 kg m^{-3} during the summers of 2014 and 2015 (Figure 3b). By summer 2016, spice anomalies within the permanent halocline returned to near normal, however the seasonal thermocline remained anomalously warm and salty. Spice anomalies during the summer 2019 MHW were minty compared to average. Minty conditions in June-July-August of 2019 were greatest within the seasonal thermocline above 25.5 kg m^{-3} (Figure 3b). As a consequence, the near surface $\Theta - S_A$ properties were much lighter compared to 2014–2016, both in winter and summer seasons. Minty conditions persisted into the winter of 2019/20.

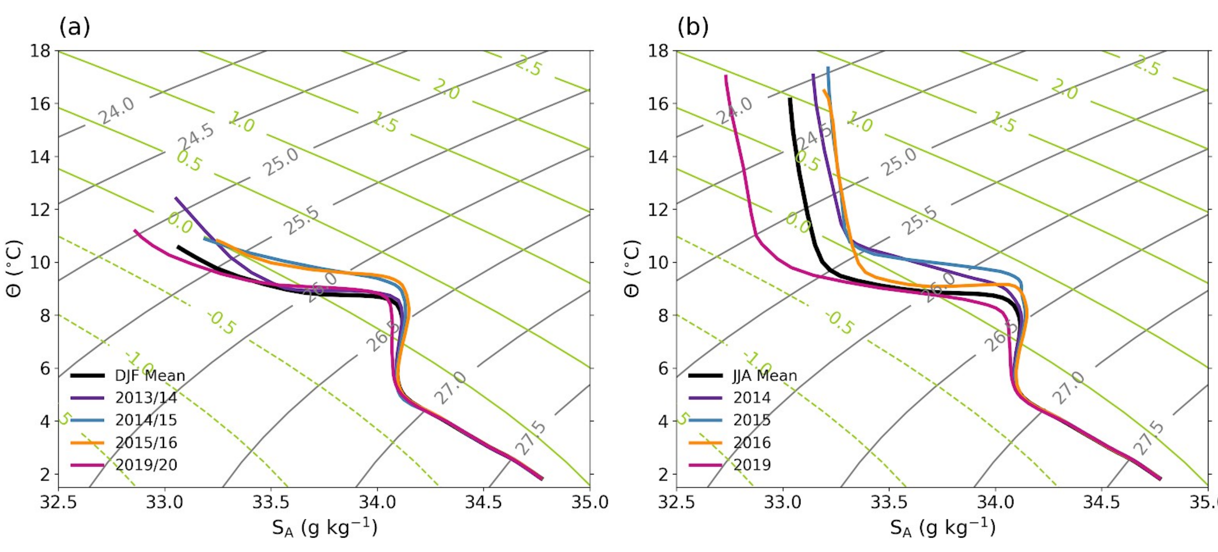

Figure 3. Winter (December-January-February) (a) and summer (June-July-August) (b) temperature-salinity relationships at 43.5ºN, 145.5ºW (lime green circles in **Figure 1**). The average 2004–2019 DJF and 2004–2019 JJA curves are shown by the thick black lines. Contours of constant spice (kg m^{-3}) in green are perpendicular to isopycnals in gray.

A connection between the evolution of surface and subsurface anomalies was a recurring theme during recent 2013–2016 and 2019–2020 NE Pacific MHWs and is visible in both Figures 2 and 4. To quantify the time lags associated with the penetrations of surface anomalies into the subsurface, we compute the lagged cross-correlation for Θ and S_A on isobars and isopycnals with values at 2.5 dbar and 25.7 kg m^{-3} respectively. Significant positive correlations between surface and subsurface $\Theta - S_A$ anomalies increase with positive lag and density between 25.7–27 kg m^{-3}. For example, the maximum cross-correlation on 26.3 kg m^{-3} occurs at 6 months positive lag (Figure S3). On the other hand, subsurface Θ anomalies (between 150–220 dbar) are most strongly correlated with the surface conditions for positive lags of 1–2 years, while subsurface S_A correlations peak at 6–12 months positive lags (Figure S3 and Figure S4).

The downward progression of surface Θ and S_A anomalies suggest that the North Pacific Ocean is capable of maintaining long-term memory of surface MHWs. One measure of memory is the heat content anomaly, Q', evaluated here over equal thickness subsurface layers. The largest Q' values occur within the seasonally varying mixed layer (10–90 dbar) where temperature fluctuations are the strongest (Figure 4). The largest positive anomalies are present during the 2013–2016 MHW. After a period of strong cooling, Q' steadily increased beginning in 2018 through present. Prior to 2013 there were two smaller MHWs that occurred in 2004–2005 and 2008–2009 that also had small gains of heat content. Evaluating Q' over deeper layers (100–180 and 200–280 dbar) reveals the persistence of Θ anomalies below the surface temperature variability. Once Θ anomalies are mixed into the subsurface, these anomalies persist even after the surface cools (Figure 4).

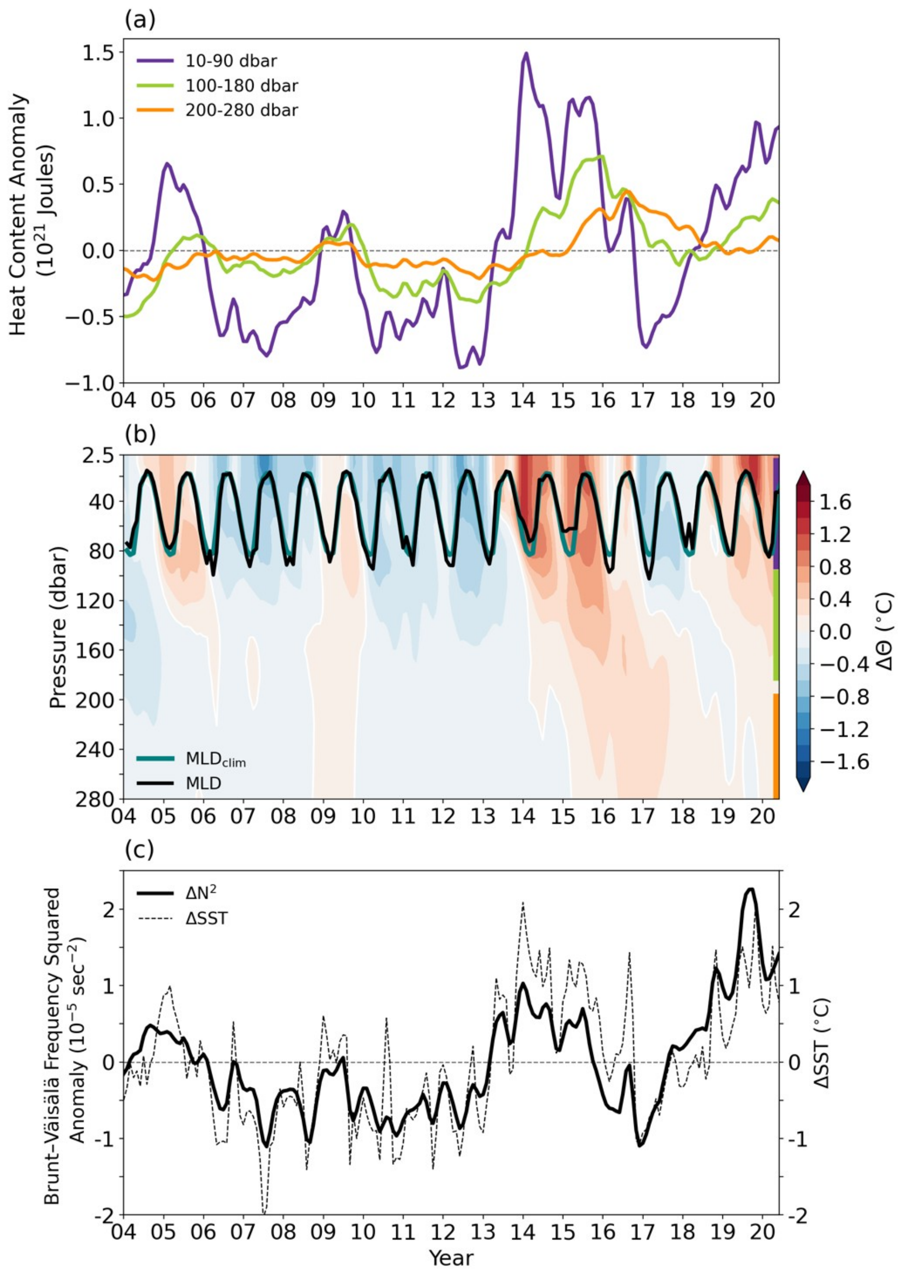

Figure 4. Variations in (a) upper ocean heat content anomalies, (b) temperature anomalies and mixed layer pressure, and (c) upper ocean stratification anomalies averaged in 35.5–51.5ºN, 135.5–154.5ºW (black outline in Figure 1). Ocean heat content anomalies are computed over three different 80-dbar pressure layers between 10–90 dbar, 100–180 dbar, and 200–280 dbar. These intervals are shown in (b) as vertical colored lines on the right hand side corresponding to (a). The mixed layer pressure and 2004-2019 climatology is computed from 19,697 Argo profiles using the Holt and Talley (2009) density algorithm. The bulk upper ocean stratification anomaly (solid lines) in (c) is computed as N^2 between 2.5 and 200 dbar and shown with the SST anomaly (dashed lines). Positive values of N^2 indicate higher water column stability and greater resistance to overturning or vertical displacement.

An increase in upper ocean heat content can affect the stability of the upper ocean. The depth of the mixed layer also shoals, which can be seen during the winters of 2013/2014 and 2014/2015 (Figure 4). The increase in stratification reduces entrainment of cool water from below and can exacerbate warming by reducing the thickness of the surface layer that accepts heat from the atmosphere, making the surface ocean easier to warm. The upper ocean stratification anomaly was noticeably higher (large N^2 anomaly values) in 2014–2015, with the largest values occurring in 2019 (Figure 4c). The very high values in 2019–2020 arise from the anomalously fresh near-surface conditions during that MHW.

5 Discussion

This study examines the evolution of subsurface $\Theta - S_A$ anomalies from Argo on both isobars and isopycnals during the 2013–2016 and 2019–2020 NE Pacific MHWs. Upper ocean salinity was anomalously fresh in the Gulf of Alaska during the 2019–2020, which greatly increased the buoyancy of the surface layer. The resulting increase in stratification in 2019–2020 likely contributed to the decrease in the depth (and density) to which water property anomalies from this event were detrained, and in places subducted. The confinement of warm anomalies to the near-surface likely enhanced the MHW's intensity.

Our results highlight important dynamical pathways for surface MHW anomalies in the NE Pacific to penetrate the subsurface; by means of detrainment, diabatic subduction, and/or adiabatic isopycnal heave. Subduction occurs in subtropical regions after temperature anomalies within the deep wintertime mixed layer detrain as a result of the mixed layer retreating in late spring. During the 2014 and 2015 spring transition of the mixed layer depth, subsurface warming occurred along both isopycnals and isobars below the mixed layer, suggesting diabatic mixing was at play for the penetration of MHW anomalies within the seasonal pycnocline. Alternatively, subsurface warming that occurs primarily on isobars and not on isopycnals was the result of heave, defined as the downward deflection of a potential density surface. We find that heave is most likely responsible for the fast appearance of anomalies below 150 dbar, for example during a 2008–2009 MHW, however the exact mechanisms of heave (i.e., from Ekman pumping due to wind stress curl) are not investigated here.

Once surface MHW anomalies are detrained out of the deep wintertime mixed layer, they can begin to propagate downward. The lag associated with the vertical propagation of surface anomalies causes the subsurface heat content to remain anomalously high even after surface conditions return to normal. This persistence of subsurface heat and the possible reemergence of surface anomalies could in fact help supercharge the occurrence of multi-year events. As future warming trends favor a more stratified upper ocean, we expect that detrainment out of the mixed layer may become less effective in storing MHW anomalies in the subsurface, and therefore further amplify surface warming. This possibility is concerning owing to the impacts that accumulated heat stress and stratification have on pelagic marine ecosystems and primary production (Smale et al, 2019; Cavole et al., 2016; Jacox et al., 2016).

Mixed layer heat budgets are frequently used to diagnose the drivers of surface warming associated with MHWs; however, the influence of salinity and subsurface water properties are often overlooked (Holbrook et al., 2020). Using the global Argo array data, this study motivates complementary analyses on the role of salinity and subsurface $\Theta - S_A$ anomalies to better understand the ocean's role in the persistence and evolution of long-lived events. Further investigation into the drivers of salinity anomalies and their role in the development of NE Pacific MHWs would appear to be a fruitful avenue of future research.

Acknowledgments and Data Availability

HAS and LT are supported by an AI for Earth Innovation Grant sponsored by the Leonardo DiCaprio Foundation and Microsoft, and wish to acknowledge cloud resources from an Azure compute grant awarded through Microsoft's AI for Earth. GCJ and JML are supported by NOAA Research and NOAA's Global Ocean Monitoring and Observing Program. HAS and SCR were also partially supported by NOAA via grant NA15OAR4320063 to the University of Washington through the Joint Institute for the Study of the Atmosphere and Ocean. This is PMEL Contribution Number 5140. The NOAA OISSTv2 dataset was provided by the NOAA/OAR/ESRL PSL, Boulder, Colorado, USA, from their Web site at https://psl.noaa.gov/. Argo data were collected and made freely available by the International Argo Program and the national programs that contribute to it (http://www.argo.ucsd.edu and http://argo.jcommops.org). The Argo Program is part of the Global Ocean Observing System.

References

Alexander, M. A., Deser, C., & Timlin, M. S. (1999), The Reemergence of SST Anomalies in the North Pacific Ocean. *Journal of Climate*, 12, 2419–2433. doi:10.1175/1520-0442(1999)012<2419:TROSAI>2.0.CO;2

Amaya, D. J., Alexander, M. A., Capotondi, A., Deser, C., Karnauskas, K. B., Miller, A. J., & Mantua, N. (in review), Are long-term changes in mixed layer depth impacting North Pacific marine heatwaves? *Bulletin of the American Meteorological Society*.

Amaya, D. J., A. J. Miller, S. Xie, & Kosaka, Y. (2020), Physical drivers of the summer 2019 North Pacific marine heatwave. *Nature Communications*, 11, 1903. doi:10.1038/s41467-020-15820-w

Bindoff, N. L., & McDougall, T. J. (1994), Diagnosing Climate Change and Ocean Ventilation Using Hydrographic Data, *Journal of Physical Oceanography*, 24, 1137-1152, doi:10.1175/1520-0485(1994)024<1137:DCCAOV>2.0.CO;2

Bond, N. A., Cronin, M. F., Freeland, H., & Mantua, N. (2015), Causes and impacts of the 2014 warm anomaly in the NE Pacific. *Geophysical Research Letters*, 42(9), 3414-3420. doi:10.1002/2015GL063306

Cavole, L. M., Demko, A. M., Diner, R. E., Giddings, A., Koester, I., Pagniello, C. M. L. S., Paulsen, M. -L., Ramirez-Valdez, A., Schwenck, S. M., Yen, N. K., Zill, M. E., & Franks, P. J. S. (2016), Biological impacts of the 2013–2015 warm-water anomaly in the Northeast Pacific: Winners, losers, and the future. *Oceanography*, 29(2), 273–285, doi:10.5670/oceanog.2016.32

Fewings, M. R. & Brown, K. S. (2019), Regional Structure in the Marine Heat Wave ofSummer 2015 Off the Western United States. *Frontiers in Marine Science*, 6, 564. doi:10.3389/fmars.2019.00564

Gentemann, C. L., Fewings, M. R. & García‐Reyes, M. (2017), Satellite sea surface temperatures along the West Coast of the United States during the 2014–2016 northeast Pacific marine heat wave. *Geophysical Research Letters*, 44, 312– 319, doi:10.1002/2016GL071039

Hobday, A. J., Alexander, L. V., Perkins, S. E., Smale, D. A., Straub, S. C., Oliver, E. C. J., Benthuysen, J. A., Burrows, M. T., Donat, M. G., Feng, M., Holbrook, N. J., Moore, P. J., Scannell, H. A., Sen Gupta, A., & Wernberg, T. (2016), A hierarchical approach to defining marine heatwaves. *Progress in Oceanography*, 141, 227-238. doi:10.1016/j.pocean.2015.12.014

Holbrook, N. J., Scannell, H. A., Sen Gupta, A, Benthuysen, J. A., Feng, M., Oliver, E. C. J., Alexander, L. V., Burrows, M. T., Donat, M. G., Hobday, A. J., Moore, P. J., Perkins-Kirkpatrick, S. E., Smale, D. A., Straub, S. C., & Wernberg, T. (2019), A global assessment of marine heatwaves and their drivers. *Nature Communications*, 10, 2624. doi:10.1038/s41467-019-10206-z

Holbrook, N. J., Sen Gupta, A., Oliver, E. C. J., Hobday, A. J., Benthuysen, J. A., Scannell, H. A., Smale, D. A., & Wernberg, T. (2020), Keeping pace with marine heatwaves, *Nature Reviews Earth & Environment*, doi.org/10.1038/s43017-020-0068-4

Holte, J. & Talley, L. (2009), A New Algorithm for Finding Mixed Layer Depths with Applications to Argo Data and Subantarctic Mode Water Formation. *Journal of Atmospheric and Oceanic Technology*, 26, 1920–1939. doi:10.1175/2009JTECHO543.1

Intergovernmental Oceanographic Commission, SCOR, and IAPSO (2010), The international thermodynamic equation of seawater – 2010: Calculation and use of thermodynamic properties, Intergovernmental Oceanographic Commission, Manuals and Guides No. 56, 196 pp., UNESCO

Jackson, J. M., Johnson, G. C., Dosser, H. V., & Ross, T. (2018), Warming from recent marine heatwave lingers in deep British Columbia fjord. *Geophysical Research Letters*, 45, 9757– 9764. doi:10.1029/2018GL078971

Jacox, M. G., Hazen, E. L., Zaba, K. D., Rudnick, D. L., Edwards, C. A., Moore, A. M. & Bograd, S. J. (2016), Impacts of the 2015–2016 El Niño on the California Current System: Early assessment and comparison to past events, *Geophysical Research Letters*, 43, 7072-7080, doi:10.1002/2016GL069716

Jayne, S.R., Roemmich, D., Zilberman, N., Riser, S. C., Johnson, K. S., Johnson, G. C., & Piotrowicz, S. R. (2017), The Argo Program: Present and future. *Oceanography*, 30(2), 18–28. doi:10.5670/oceanog.2017.213

McDougall, T. J., & Krzysik, O. A. (2015), Spiciness, *Journal of Marine Research*, 73, 141-152, doi:10.1357/002224015816665589

Munk, W., 1981: Internal waves and small-scale processes. *Evolution of Physical Oceanography*, B. A. Warren and C. Wunsch, Eds., MIT Press, 264–291

Oliver, E. C. J., Donat, M. G., Burrows, M. T., Moore, P. J., Smale, D. A., Alexander, L. V., Benthuysen, J. A., Feng, M., Sen Gupta, A., Hobday, A. J., Holbrook, N. J., Perkins-Kirkpatrick, S. E., Scannell, H. A., Straub, S. C. & Wernberg, T. (2018), Longer and more frequent marine heatwaves over the past century, *Nature Communications*, 9, 1324, doi:10.1038/s41467-018-03732-9

Qiu, B., & Huang, R. X. (1995), Ventilation of the North Atlantic and North Pacific: Subductions Versus Obduction, *Journal of Physical Oceanography*, 25, 2374-2390, doi:10.1175/1520-0485(1995)025<2374:VOTNAA>2.0.CO;2

Reynolds, R. W., Smith, T. M., Liu, C., Chelton, D. B., Casey, K. S. & Schlax, M. G. (2007), Daily High-Resolution-Blended Analyses for Sea Surface Temperature, *Journal of Climate,* 20, 5473-5496, doi:10.1175/2007JCLI1824.1

Reynolds, R. W., Rayner, N. A., Smith, T. M., Stokes, D. C. & Wang W. (2002), An improved in situ and satellite SST analysis for climate, *Journal of Climate*, 15, 1609-1625, doi:10.1175/1520-0442(2002)015<1609:AIISAS>2.0.CO;2

Roemmich, D. & Gilson, J. (2009), The 2004-2008 mean and annual cycle of temperature, salinity, and steric height in the global ocean from the Argo Program, *Progress in Oceanography*, 82, 81-100, doi:10.1016/j.pocean.2009.03.004

Schmeisser, L., Bond, N. A., Siedlecki, S.A., & Ackerman, T. P. (2019), The role of clouds and surface heat fluxes in the maintenance of the 2013–2016 Northeast Pacific marine heatwave, *Journal of Geophysical Research: Atmospheres*, 124, 10772-10783, doi:10.1029/2019JD030780

Smale, D. A., Wernberg, T., Oliver, E. C. J., Thomsen, M., Harvey, B. P., Straub, S. C., Burrows, M. T., Alexander, L. V., Benthuysen, J. A., Donat, M. G., Feng, M., Hobday, A. J., Holbrook, N. J., Perkins-Kirkpatrick, S. E., Scannell, H. A., Sen Gupta, A., Payne, B. L. & Moore, P. J. (2019), Marine heatwaves threaten global biodiversity and the provision of ecosystem services, *Nature Climate Change*, 9, 306-312, doi:10.1038/s41558-019-0412-1

Zaba, K. D. & Rudnick, D. L. (2016), The 2014–2015 warming anomaly in the Southern California Current System observed by underwater gliders. *Geophysical Research Letters*, 43, 1241-1248, doi:10.1002/2015GL067550